Electronic Supplementary Information

Efficient arsenic coagulation by serpentine mediated iron hydroxides

Lei Ouyang, [a] Fangfang Song, [a] Caiyue Yu, [a] Lijin Huang, [a] Qin Shuai, [a,*]

[a] State Key Laboratory of Biogeology and Environmental Geology, Faculty of Materials Science and Chemistry, China University of Geosciences, Wuhan 430074, China.

Author contributions, Experimental section, Table S1, Fig. S1-S7 are included.

Author contributions

L. Ouyang: conceptualization, investigation, writing – original draft. F. Song: methodology, formal analysis. C. Yu: investigation. L. Huang: writing – review and editing. Q. Shuai: supervision, funding acquisition, writing – review and editing.

Experimental Section

Chemical reagents

Disodium hydrogen arsenate heptahydrate ($Na_2HAsO_4 \cdot 7H_2O$, ≥ 98%), sodium arsenite ($NaAsO_2$, AR), ferrous sulfate heptahydrate ($FeSO_4 \cdot 7H_2O$, AR), iron sulfate ($Fe_2(SO_4)_3$, AR), magnesium carbonate ($MgCO_3$, AR), magnesium oxide (MgO, SP), magnesium silicate ($MgSiO_3$, 60-80 mesh), hydrochloric acid (HCl, AR), nitric acid (HNO_3, GR) were purchased from Sinopharm Reagent Shanghai Co., Ltd (China). The water used in this study is deionized water with conductivity of 18.2 MΩ·cm. The serpentine powder used in the experiment was purchased from Chongqing Dongfeng Chemical Plant (China) with particle size of 200 meshes. Its main chemical composition can be found in Table S1 shown below. The firing weight loss was calculated by the weight loss after the serpentine sample was burned in a muffle furnace at 1000 ℃ for 2h.

Table 1 Chemical composition of the serpentine determined by XRF

Composition	wt/ %	Composition	wt/ %
MgO	35.0	MnO	0.10
SiO_2	40.1	K_2O	0.05
Fe_2O_3	6.90	Na_2O	0.03
CaO	1.50	TiO_2	0.01
Al_2O_3	0.70	P_2O_5	0.01
Firing weight loss	15.1		

Characterization methods and instruments

The morphology and elemental distribution of serpentine and sediments after coagulation was observed by transmission electron microscope (TEM: Talos F200x, Thermo Fisher Scientific) with Energy Dispersive Spectrometer (EDS). The crystal structure was analyzed by X-ray diffractometer (XRD: SmartLab SE, Rigaku, Japan). Fourier transform infrared spectra were obtained by Fourier

transform infrared spectrometer (FT-IR: Nicolet iS50, Thermo Fisher Scientific, USA). X-ray photoelectron spectroscopy (XPS: K-Alpha, Thermo Fisher Scientific, USA) was used to obtain the information of valence change. The As concentration in the solution was determined by inductively coupled plasma emission spectrometer (ICP-OES: EXPEC 6000, EXPEC Technology, China). The arsenic removal efficiency is calculated as follows:

$$R = \frac{c_I - c_R}{c_I} \times 100\ \%$$

Wherein, R represents the arsenic removal rate (%), c_I represents the initial concentration of arsenic ion (mg/L), and c_R represents the ion concentration after reaction (mg/L).

Coagulation experiment

Initial As solution (100 mL) was diluted from As stock solution, the pH value was adjust to around 7. Certain amount of serpentine powder and ferrous sulfate heptahydrate are dispersed into the solution based on the molar ratio. The mixture was moved to a thermostatic oscillator (SHA-B, Guohua, China) for coagulation. Stir speed and temperature were set to 170 r/min and 25 ℃, respectively. After reaction for a certain period of time, part of the mixture was obtained with a syringe, and filter with a filter (polyethersulfone, pore diameter 0.45 μm). The supernatant was sampled for As concentration determination.

Raman characterization with SHINERS method

Raman spectra were received on a Raman spectrometer (RISE, WITec, Germany) coupled with a *in situ* Raman cell (EC-Raman, Beijing Scistar Technology Co. Ltd, China). To promote the characterization sensitivity, SiO_2 shell isolated Ag@Au NPs were used as the Raman signal enhancer. The detail synthesis method can be found in our recent work (*Nano Research*, 2023, 16(2): 3046-3054). The serpentine and sediments after arsenic coagulation was mixed with SiO_2 shell isolated Ag@Au NPs and drip-coated onto the electrode in the Raman cell before Raman monitoring. Ten spectra were obtained at random chose positions for each sample. The averaged spectrum was used for analysis.

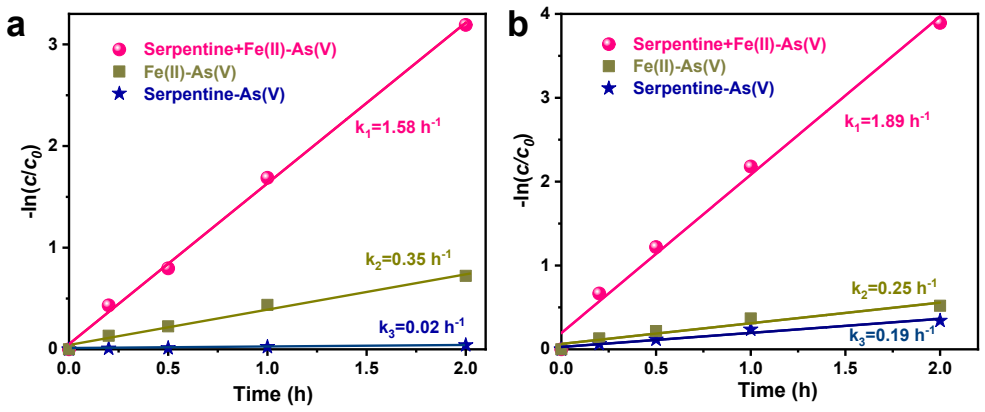

Fig. S1 Removal kinetics of (a) As(V) and (b) As(III) during the serpentine-Fe(II) coagulation process, respectively. Arsenic initial concentration 30 mg·L^{-1} (100 mL).

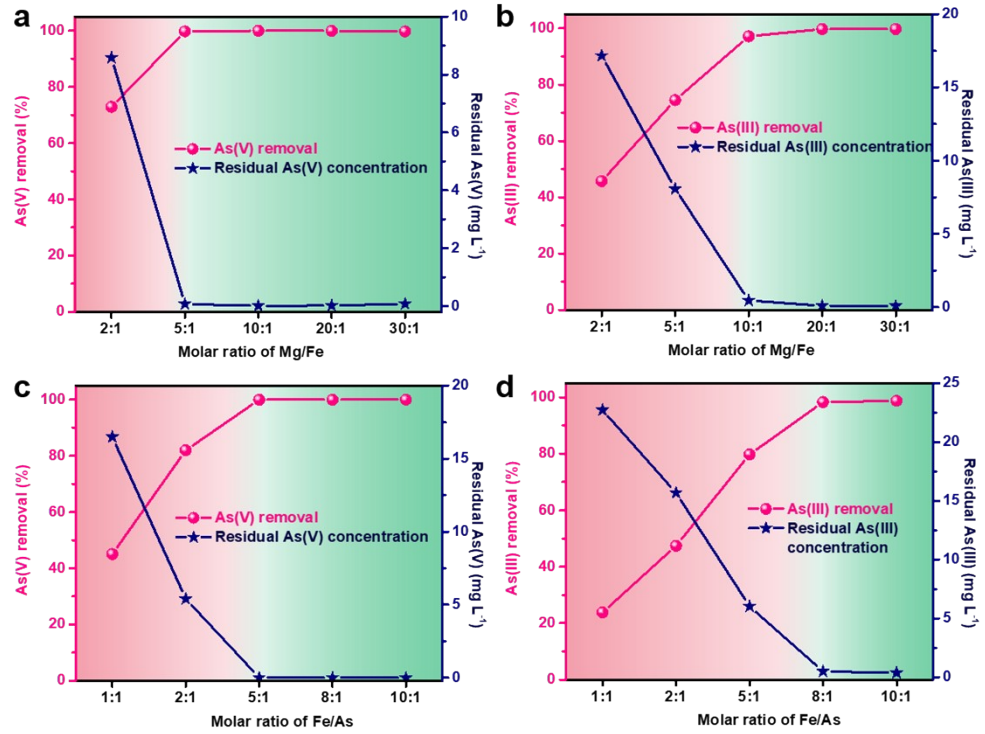

Fig. S2 Dosage optimization for serpentine and Fe(II). The removal efficiency and residue concentration of (a) As(V) and (b) As(III) with different dosages of serpentine. The removal efficiency and residue concentration of (c) As(V) and (d) As(III) with different dosages of Fe(II). Arsenic initial concentration 30 mg·L^{-1} (100 mL).

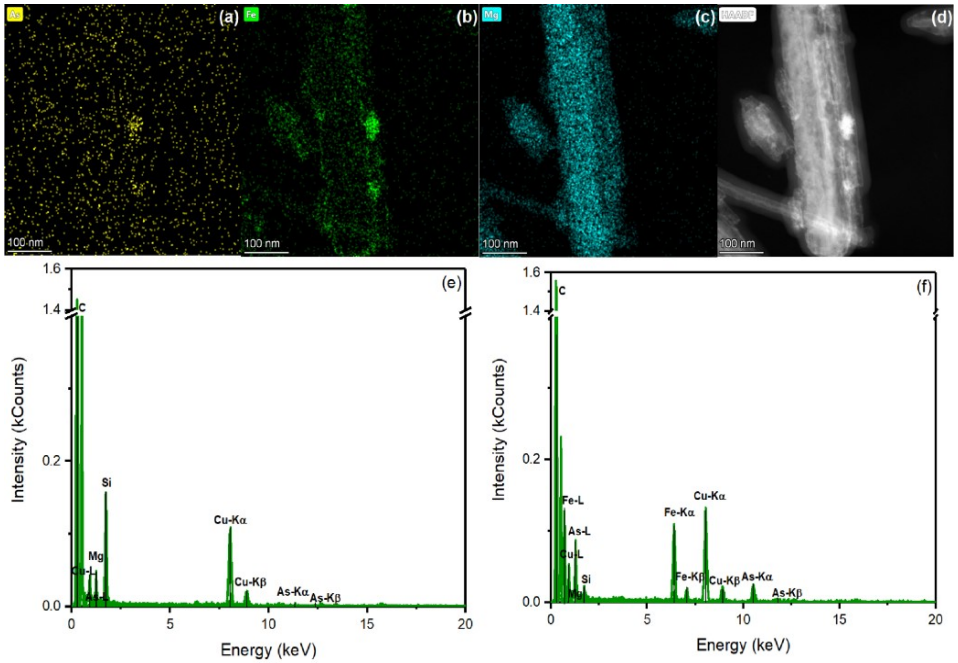

Fig. S3 Elemental distribution (a-d) and EDS spectra (e, f) of sediments of As(V) after serpentine-Fe(II) coagulation. The detected Cu element came from the copper mesh for sample preparation.

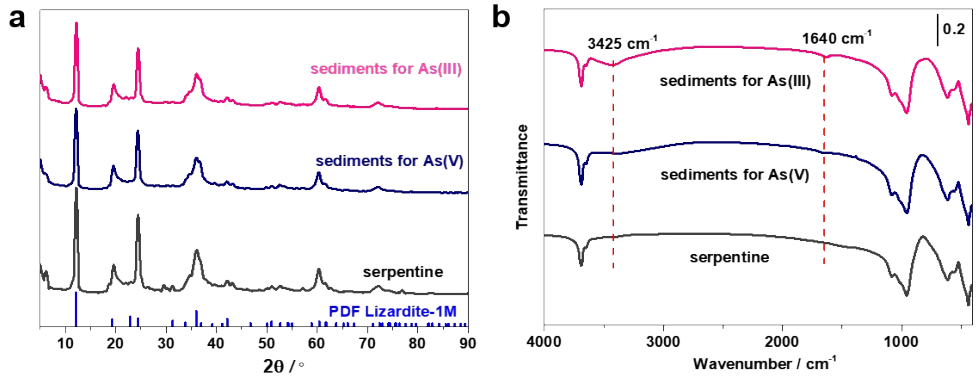

Fig. S4 (a) XRD pattern and (b) FT-IR spectra of serpentine and sediments after arsenic coagulation.

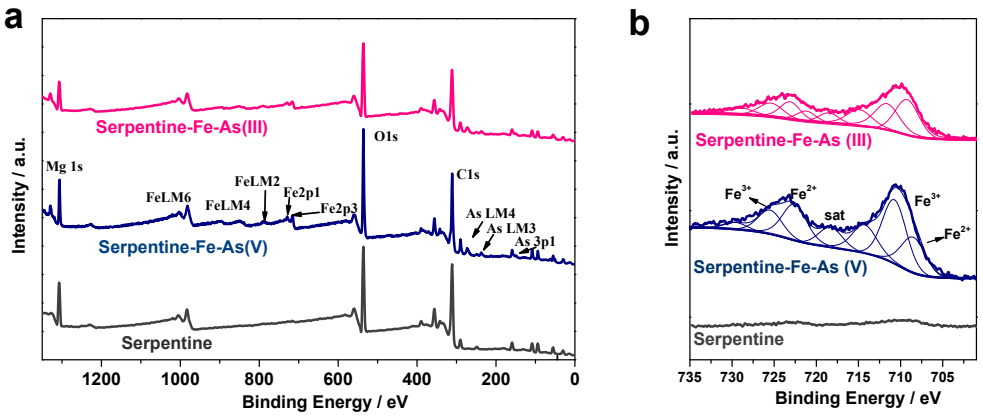

Fig. S5 XPS spectra of serpentine and sediments after arsenic coagulation. (a) Full spectra. (b) High-

resolution Fe 2p spectra.

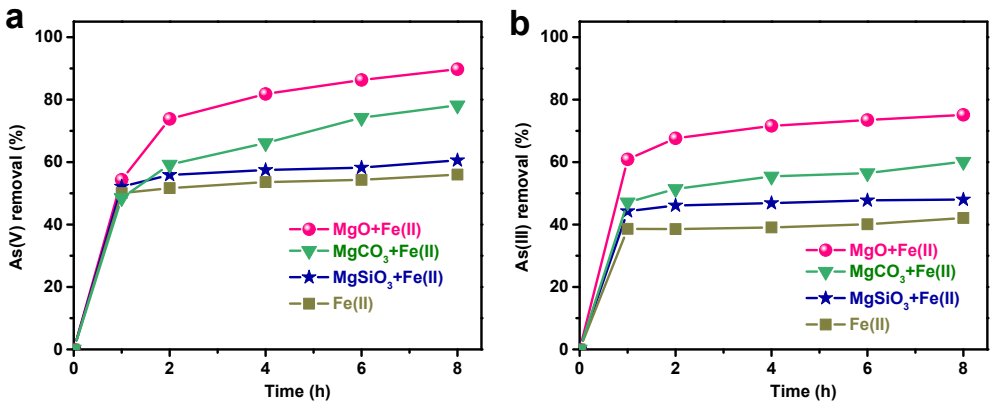

Fig. S6 (a) As(V) and (b) As(III) coagulation performance of magnesium compounds with Fe(II) including MgO, $MgCO_3$ and $MgSiO_3$, respectively.

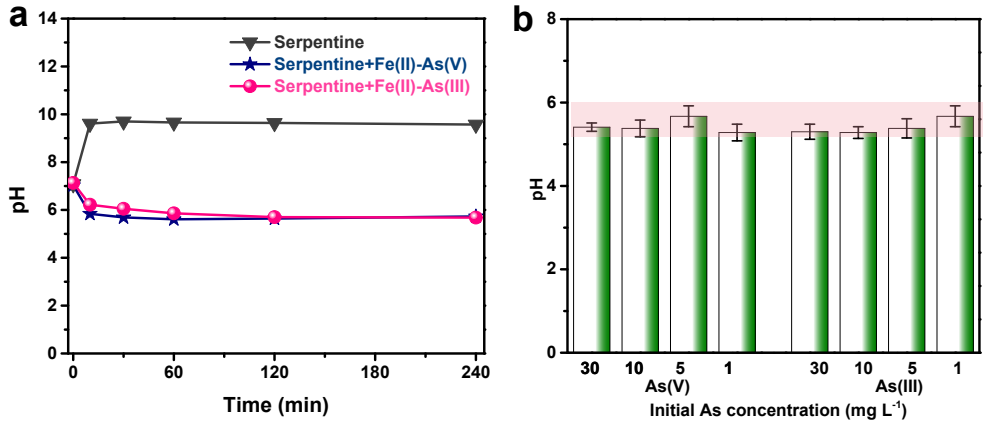

Fig. S7 pH buffering ability of serpentine. (a) The time dependent pH value of the dispersion of serpentine and during the arsenic coagulation process. (b) The pH values of the dispersion after arsenic coagulation with different initial arsenic concentrations.